## EFFECT OF EXTERNAL TURBULENCE ON SEDIMENT PICKUP RATE

Akio Okayasu<sup>1</sup>, Keiichiro Fujii<sup>2</sup> and Masahiko Isobe<sup>2</sup>

Influence of turbulence on sediment pickup rate was investigated. Pickup rates with external turbulence generated by a grid structure were measured in a channel. It was found that the rates were much larger than those for non-turbulent conditions. A new formula in which external turbulence was taken into account for Shields parameter evaluation was proposed. In the formula, effect of inertia force by turbulence acting on sediment particles was included as well as the enlarged drag force caused by fluctuating velocity.

Keywords: pickup function; external turbulence; Shields parameter; wave breaking; sediment transport

#### INTRODUCTION

For predicting beach topography change, accurate evaluation of sediment movement under wave motion is important. With numerical flow simulations, sediment transport in unsteady flows under wave action is now often calculated as an advection-diffusion process (e.g. Suzuki et al. 2007), in which the source term (re-suspension term) is commonly evaluated by the pickup function proposed by van Rijn (1984) and Nielsen (1992). Nadaoka et al. (1988), however, pointed out that in the surfzone, turbulence generated by wave breaking affects the rate of sediment re-suspension, which means the pickup rate should be influenced by external turbulence transported from the upper layer.

As for the bottom shear stress under turbulence, some laboratory experiments have been done. Cheng et al. (2003) performed bottom shear stress measurement under uniform flows in a flume with turbulence generating grids and found that bed shear stress fluctuated markedly in comparison with those for the condition of plain uniform channel flows or boundary layers. Sumi et al. (2009) measured bottom shear stress under spilling breakers on a slope. They described that the shear stress under wave breaking was different from that evaluated by the wave theory, while shear stress under non-breaking waves agreed to that.

Those experimental results suggest that sediment pickup rate under wave breaking condition is different from that proposed for plain flows without external turbulence. The non-linear form of the pickup functions also shows that fluctuating component of velocity (or local shear stress) should affect the calculated pickup. The purpose of this study is to investigate the influence of the turbulence to the pickup rate through a laboratory experiment. The sediment pickup rates were compared among cases with and without the external turbulence generated by a grid structure in a uniform channel flow.

# **EXPERIMENT**

# **Experimental Setup and Conditions**

A 25 m long and 0.5 m wide uniform flow flume was used for the experiment. Figure 1 shows a schematic figure of the flume and experimental setup. In the downstream part of the flume, the original flume floor was ascended 50 mm by a flat fixed bed, which gradually descended by a -1/10 slope at the last part. In order to give artificial roughness on the surface, sand ( $d_{50}$ =0.31 mm) was glued on the bed. On the descending part, the same sand was put (not glued) as a movable bed so as to make a horizontal bed at the beginning of each measurement. Flow was generated by a recirculating pump system, and the flow velocity was adjusted by changing flow rate and position of a gate installed at the end of the flume. Water depth on the fixed bed part was maintained to be about 40 cm.

Change of bed elevation at the movable sand bed was precisely measured by a laser distance meter (Keyence, LK-G505) at 10 cm downstream of the initial border of the fixed and movable bed sections as shown in Fig. 2. The size of the measured area (laser spot) was 0.30 mm (longitudinal direction) by 9.5 mm (transverse direction) and the sensor gave an average distance to the target within an error range of  $\pm 0.1$  mm which was small enough to measure surface elevation change of 0.31 mm diameter sand. In order to prevent refraction and reflection at the water surface, the laser beam of the distance

Department of Ocean Sciences, Tokyo University of Marine Science and Technology, 4-5-7, Konan, Minato-ku, Tokyo 108-8477, Japan

<sup>&</sup>lt;sup>2</sup> Graduate School of Frontier Sciences, University of Tokyo, 5-1-5 Kashiwanoha, Kashiwa-shi, Chiba 277-8563,

meter was put from the glass sidewall and reflected by a mirror to be perpendicular to the initial sand bed.

Longitudinal (downstreamwise) velocity was simultaneously measured by a laser Doppler velocimeter (LDV; Dantec, FiberFlow) at 10 mm above the initial bed level. The transverse distance of the measuring point was 180 mm from the glass sidewall as shown in Fig. 3. The laser distance meter aimed the sand bed just below the velocity measuring point. Variation of averaged flow velocity at 10 mm above the bottom in the transverse direction is given in Fig. 4. As shown in the figure, influence of the glass sidewall was limited within the distance of 30 mm from the wall.

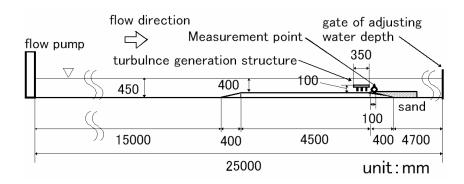


Figure 1. Experimental set-up.

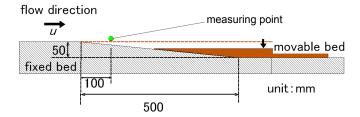


Figure 2. Close-up of movable bed section.

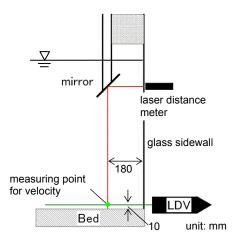


Figure 3. Arrangement for measurements of bottom elevation and flow velocity in the transverse and vertical plane. Red line shows measuring line of surface elevation, green dot is the measuring point of longitudinal velocity.

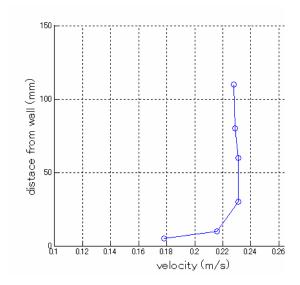


Figure 4. Variation of time-averaged longitudinal flow velocity in the transverse direction.

The experiment was conducted for 8 cases; 4 cases were for non-turbulent conditions and the other 4 cases were for turbulent conditions. The experimental conditions are listed in Table 1. The flow rate and gate height were adjusted to achieve the target Shields parameter with a constant water depth of 40 cm. For non-turbulent cases, the flow was not supposed to be laminar because of usual boundary generated turbulences (typical Reynolds number of the flow:  $2 \times 10^5$ ). The term "non-turbulent" here means flow observed in an ordinary plain channel.

Table 1. Experimental conditions.

| Cas | Grid structure | θ   | Q (m <sup>3</sup> /s) | Gate height (mm) |
|-----|----------------|-----|-----------------------|------------------|
| е   |                |     |                       |                  |
| 1   | Without        | 0.3 | 5.00                  | 380              |
| 2   | Without        | 0.6 | 6.20                  | 340              |
| 3   | Without        | 0.9 | 7.00                  | 290              |
| 4   | Without        | 1.2 | 7.50                  | 270              |
| 5   | With           | 0.3 | 5.30                  | 330              |
| 6   | With           | 0.6 | 6.50                  | 300              |
| 7   | With           | 0.9 | 7.50                  | 270              |
| 8   | With           | 1.2 | 8.50                  | 260              |

(θ: Target Shields parameter, Q: Flow rate)

For the turbulent cases, excess turbulence was artificially generated by a grid structure shown in Fig. 5. As shown in Fig. 1, it was placed so as the end of the structure to be at the end of the fixed bed section. The clearance between the fixed bed floor and lower end of the structure was 15 mm, while the effective structure height (length of the rectangular columns) was 100 mm.

With this grid structure, property of generated turbulence was considered to have variation along the flow direction in the movable bed section. Therefore, uniformity of turbulence in the longitudinal direction was not assumed in the present study. Instead, correlation was investigated between change of the bed level and flow properties measured just above the target position.

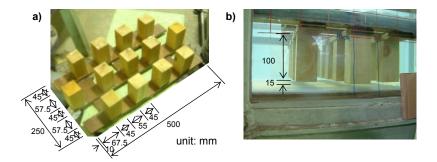


Figure 5. Turbulence generating grids installed at upstream of measuring section.
a) grid structure made of wood, b) grid set in the flume.

# **Data Acquisition and Analysis**

The measurements were done five times for each case. Each measurement was started from still water condition with regulated height of the end gate. Bed elevation and velocity were recorded for 110 s from 30 s after the start of pump system. The LDV system used in the present study gave velocity records at uneven intervals. In order to obtain sufficiently high frequency resolution for velocity data, measurements with less than 500 data per second during distinct change of the bed level were discarded. After measurements, velocity records were resampled to data at even intervals of 500 Hz for further analysis.

Figure 2 shows an example (case 2-2: the second record of the case 2) of time series of velocity, bed level, and pickup rate. The pickup rate was evaluated as a differential of the bed level change and expressed as a blue line in the bottom panel of the figure. The red line in the panel shows pickup rate calculated by Nielsen's formula (1992) from the measured velocity moving-averaged for every 0.1 s.

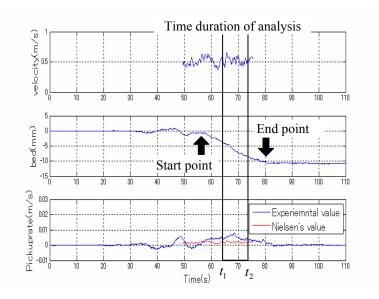


Figure 6. Time series of velocity, bed level, and pickup rate (case 2-2).

The Nielsen's formula is the unsteady version of van Rijn's (1984), and is given by

$$p = 0.00033 \left( \frac{\theta' - \theta_c}{\theta_c} \right)^{1.5} \frac{(s-1)^{0.6} g^{0.6} d^{0.8}}{v^{0.2}}$$
 (1)

where p is the pickup rate,  $\theta'$  the effective Shields parameter,  $\theta_c$  the critical Shields parameter (= 0.05 in the present study), s the relative density of sediment, g the acceleration due to gravity, d the sediment diameter,  $\nu$  the kinematic viscosity of water. The effective Shields parameter is calculated in this study as

$$\theta' = \frac{\tau}{W} \tag{2}$$

where  $\tau$  is the shear stress on a sediment particle and W the gravitational force.  $\tau$  is estimated as the drag force on sediment particles and expressed by

$$\tau = \frac{1}{2} C_D \rho \frac{\pi d^2}{4} u_b^2$$
 (3)

where  $C_D$  is the drag coefficient and is given by

$$C_D = \frac{24}{Re} \left( 1 + 0.15 Re^{0.687} \right)$$
 for  $Re < 1000$  (4)

where Re is the particle Reynolds number for the sediment and was less than 1000 for the present study.  $\rho$  is the density of water and  $u_b$  is the friction velocity calculated from the measured velocity u as

$$u_b = \frac{\kappa}{\ln\left(\frac{30.1z}{d}\right)}u\tag{5}$$

where  $\kappa$  is the Karman constant, z the height of the velocity measuring point from the bed. Since W is evaluated by

$$W = g(\rho_s - \rho) \frac{\pi d^3}{6} \tag{6}$$

where  $\rho_s$  is the density of sediment particle, the effective Shields parameter can be rewritten as

$$\theta' = \frac{3}{4} C_D \frac{u_b^2}{(s-1)gd} \tag{7}$$

For evaluation of pickup rate, data at the middle of distinct bed level change were used. As shown in Fig. 6, the bed level didn't change until a certain moment (time  $t = 30 \, \text{s}$  in the case for Fig. 6). It can be considered as spin-up time for the main flow including the period of another 30 seconds before the data acquisition. After  $t = 30 \, \text{s}$ , the bed level changed unsteadily, which showed unsteadiness of flow state and effect of sediment movement in the upstream part of the target position. From  $t = 57 \, \text{s}$  to  $t = 80 \, \text{s}$ , the bed was steadily descending and the calculated pickup rate was rather stable. Since it was considered that the steadily descending period showed stability of the flow and minor influence of sediment in the upstream part, data within  $\pm 5 \, \text{seconds}$  of the center of this period were used for analysis. In some cases when the pickup rate was too large to have enough length of time, the duration was less than 10 seconds, but more than 6 seconds.

# **EXPERIMENTAL RESULTS**

# Reliability of Pickup Rate Evaluation by means of Bed Level Change

A comparison between time-averaged values of pickup rates obtained from measured bed elevation and those evaluated by Eq. (1) from time-averaged velocity was given in Fig. 7 for the non-turbulent cases. Although some scattering can be seen, the experimental values agree well with the Nielsen's (van Rijn's) values and plots are around the 1:1 line. Since the van Rijn's experiment was conducted under non-turbulent (without excess turbulence) conditions and the coefficient in Eq. (1)

was based on its results, the figure indirectly shows the reliability of the present method for pickup rate evaluation.

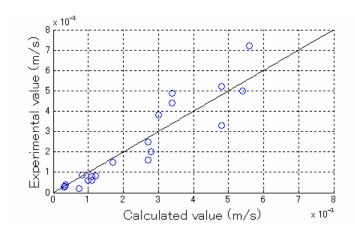


Figure 7. Measured pickup rate for non-turbulent cases.

# **Turbulence Property and Pickup Rate**

Figure 8 gives an example of velocity variations for non-turbulent and turbulent cases for the same target Shields parameter. As shown in the figure, fluctuation was much larger in the turbulent case. Since the mean velocities are almost the same, time-averaged Shields parameter should be the same.

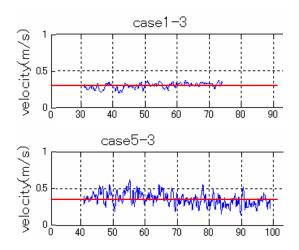


Figure 8. Measured velocity records for non-turbulent case (top) and turbulent case (bottom).

Non-dimensional turbulence intensity  $T_I$  was calculated for each case as

$$T_I = \frac{\sqrt{\left(\sum_{i=1}^n u'^2\right)/n}}{\overline{u}} \tag{8}$$

where u' is the turbulent component of velocity,  $\overline{u}$  the time-averaged velocity and n the number of the data. Relation between non-dimensional turbulence intensity and Shields parameter is plotted in Fig. 9. The figure indicates that non-dimensional turbulence intensities for the turbulent conditions

were about twice as large as those for the non-turbulent conditions. Power spectra suggest that the primary source of turbulence energy is in frequency of 1 to 3 Hz. (Fig. 10)

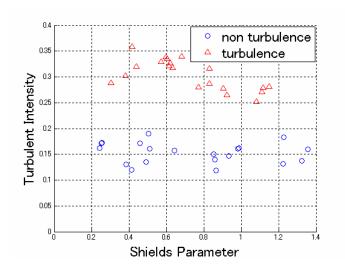


Figure 9. Non-dimensional turbulent intensities for non-turbulent and turbulent conditions.

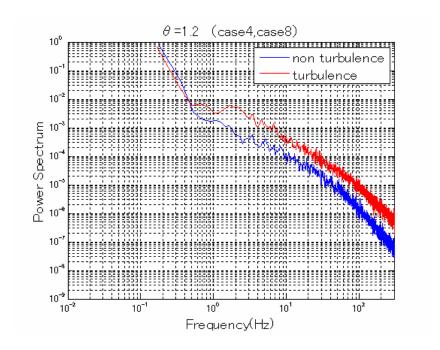


Figure 10. Power spectra of measured velocity for not-turbulent case (blue; case 4) and turbulent case (red; case 8).

Figure 11 shows relation between Shields parameter evaluated from time-averaged velocity and the measured pickup rates for all cases. The solid line in the figure indicates values evaluated by Eq. (1). It is found from the figure that the Nielsen's formula underestimates the pickup rates for the turbulent conditions, and the measured values are almost three times larger. This result suggests that the turbulence exerts a great influence on sediment pickup and should be taken into account in some way for evaluation of pickup rate under excess turbulence.

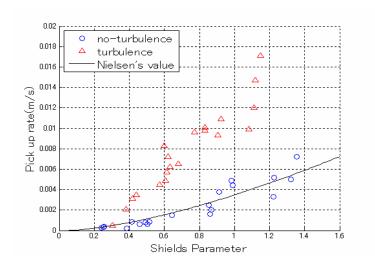


Figure 11. Relation between Shields parameter and pickup rates.

As it is qualitatively expected from the form of Eq. (1) which is nonlinear to the velocity, turbulent component of the velocity may largely affect the evaluation of the pickup rate. Figure 12 is response of calculated pickup rates against calculation frequency of velocity averaging. The blue circles show relative pickup rates for non-turbulent cases compared to a value calculated by Eq. (1) for velocity averaged over 10 s. The value at 10<sup>0</sup> Hz gives a mean value of 10 pickup rates calculated by using velocities averaged every 1 s. The values are averaged over the all non-turbulent cases. The red triangles show values for the turbulent cases.

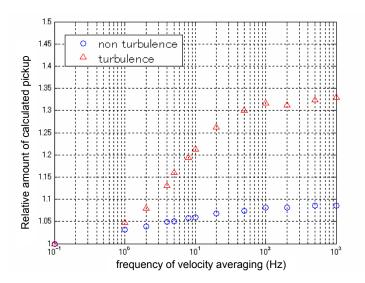


Figure 12. Response of calculated pickup rates against calculation frequency of velocity averaging (blue: non-turbulent case, red: turbulent case).

It is shown in the figure that if the sampling frequency is higher, the calculated pickup rates become larger. The increment is up to 30% for the turbulent cases, but it is less than 10 % for the non-turbulent cases. The result means, however, that the simple effect of turbulence through the non-linearity of Eq. (1) is not enough to explain the increment of pickup rates measured for the turbulent cases, and some other mechanism should be considered to improve the applicability of the evaluation

method. In the next section, force balance on a sediment particle is reconsidered to develop a new formula for pickup rate evaluation.

### PICKUP RATE EVALUATION UNDER EXCESS TURBULENCE

#### **Formulation of Modified Shields Parameter**

Since it was shown in the previous section that Eq. (1) could estimate the pickup rate reasonably well for non-turbulent conditions and only one sediment diameter was tested in the experiment, the form of Eq. (1) is left untouched for extension to cases with turbulence. Instead, in order to take the effect of excess turbulence into account, a new formula is proposed for evaluation of Shields parameter. In the new formulation, Eq. (1) is rewritten by using the modified Shields parameter  $\theta_t$  as,

$$p = 0.00033 \left(\frac{\theta_t - \theta_c}{\theta_c}\right)^{1.5} \frac{(s-1)^{0.6} g^{0.6} d^{0.8}}{v^{0.2}}$$
(9)

$$\theta_t = \frac{F_D + F_I}{W - F_L} \tag{10}$$

where  $F_D$  is the drag force,  $F_I$  the inertia force, W the gravitational force and  $F_L$  the lift force acting on a sediment particle including turbulence effect.

A schematic illustration of the forces acting on a particle on the bed is given in Fig. 13. Shear stress  $\tau$  in a general expression for Shields number, Eq. (2), is here described as a summation of drag force and inertia force which may not be negligible in a high frequency of velocity fluctuation. Also, lift force may play a certain role on the net weight of particles under high frequency flow motion.

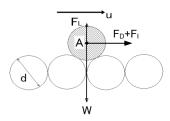


Figure 13. Schematic figure of forces acting on a sediment particle in a flow.

In the present study, drag force  $F_D$  is evaluated by the following equation same as Eq. (3) as

$$F_D = \frac{1}{2} C_D \rho \frac{\pi d^2}{4} u_{bl}^2 \tag{11}$$

where  $u_{bt}$  the bottom shear velocity including the turbulence component.  $C_D$  is evaluated by Eq. (4). The bottom shear velocity is estimated by

$$u_{bt} = \frac{\kappa}{\ln\left(\frac{30.1z}{d}\right)} \left(\overline{u} + 1.41u'_{rms}\right) \tag{12}$$

where  $u'_{rms}$  the root-mean-square value of turbulence component of the measured velocity. The factor 1.41 is derived under assumption of isotropic turbulence in the horizontal 2-D plane. It should be noted here that  $u'_{rms}$  is calculated from resampled data for a certain frequency which is obtained by

averaging the original velocity data over a corresponding time interval. It is therefore  $u'_{rms} = 0$  and  $u_{bt}$  is the same as the original shear stress  $u_b$  in Eq. (3) for complete steady flow assumption.

The inertia force is evaluated by the following equation by using time derivatives of  $u_b$  as

$$F_I = C_I \rho \frac{\pi d^3}{6} \frac{du_b}{dt} \tag{13}$$

where  $C_I$  is the inertia coefficient and was taken to be 1.5 for this study. The time derivatives of velocity can be estimated from the measured velocity data, but in the present study the following procedure is proposed for practical applications and numerical simulations. Time derivatives of bottom shear velocity can be denoted as

$$\frac{du_b}{dt} = u_b \frac{U}{L} \tag{14}$$

where U is the representative velocity, L the representative length of turbulence. Substituting

$$U = \sqrt{K} = \sqrt{\frac{1}{2}\overline{u'u'}}, \ L = C_{\mu}f_{\mu}\frac{K^{\frac{3}{2}}}{\varepsilon}$$
 (15)

obtained for the  $K - \varepsilon$  model at low Reynolds number after Jones and Launder (1972) into Eq. (14),

$$\frac{du_b}{dt} = u_b \frac{f}{C_\mu f_\mu} \tag{16}$$

is derived, where K is the turbulence kinetic energy and  $\varepsilon$  the energy dissipation rate of the turbulence. Further, the model coefficients  $C_{\mu}$  and  $f_{\mu}$  are given as

$$C_{\mu} = 0.09$$
,  $f_{\mu} = \exp\left(\frac{-2.5}{1 + R_t/50}\right)$ ,  $R_t = \frac{K^2}{v\varepsilon}$ . (17)

In the present study, the energy dissipation rate  $\varepsilon$  is evaluated in a rather simple way that

$$\varepsilon = A f_{\rho} U^2 \tag{18}$$

where A is a constant assumed to be 1, and  $f_e$  the representative frequency of eddies that is assumed as

$$f_e = St \frac{\overline{u}}{d_s} \tag{19}$$

where St is Strouhal number and set to be 0.2 for this case, and  $d_s$  the representative length of turbulence generating objects and the width of the rectangular columns of the grid structure is substituted.

Finally, the lift force is evaluated as

$$F_L = \frac{1}{2} C_L \rho \frac{\pi d^2}{4} u_{bt}^2, \tag{20}$$

where  $C_L$  is the lift coefficient and was assumed to be 0.2 for the present cases.

Figure 14 gives a comparison between pickup rates obtained from the bottom elevation change and those calculated by Eq. (9) with Eq. (10) for evaluation of the modified Shields parameter. In the figure, calculated pickup rates show larger values in the region of relatively small pickup rates, i.e., small Shields number. It is, however, found that the measured and calculated values are plotted around the line 1:1 for both non-turbulent and turbulent cases, and can be concluded that the estimation is much improved.

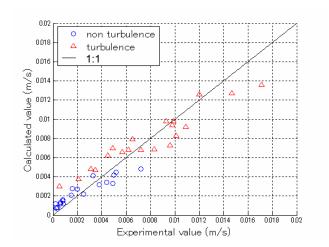


Figure 14. Comparison of pickup rates between experimental values and values calculated with proposed Eq. (8).

In order to see the effects of turbulent velocity term in Eq. (12) and inertia force Eq. (13) to the modified Shields parameter Eq. (10), each contribution to the pickup rates are investigated. Figure 15 shows pickup rates for the turbulent conditions with and without the turbulent velocity and the inertia force. It is found that the major contribution is given by the turbulent velocity part, and the effect of the inertia force is not negligible, but minor.

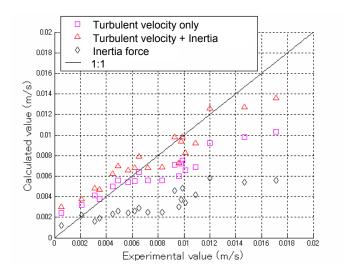


Figure 15. Contributions of each factor for evaluating Eq. (9).

### Formulation for Instantaneous Velocity

For cases that high frequency velocity measurement is achieved or for numerical flow simulations with very fine time resolution such as the direct numerical simulations, the turbulence effect can be directly evaluated for the pickup rate calculation. For these cases, Eq. (12) can be replaced by

$$u_{bt} = \frac{\kappa}{\ln\left(\frac{30.1z}{d}\right)}u\tag{21}$$

where u is the instantaneous velocity. Eq. (16) is also replaced by using instantaneous velocity as

$$\frac{du_b}{dt} = \frac{u(i) - u(i-1)}{\Delta t} \tag{22}$$

where u(i) is the i th record of velocity and  $\Delta t$  the time interval of velocity data.

Figure 16 shows a comparison between pickup rates evaluated from the bottom level change and those calculated by Eq. (9) with Eqs. (21) and (22) for the measured instantaneous velocity data. Although the calculated values are slightly larger than those shown in Fig. 14, the agreement is generally good. It can be thus concluded that a set of Eqs. (6), (9) to (13) and (16) to (20) can be used for evaluation of pickup rate if the turbulence property is given, and another set of Eqs. (6), (9), (10), (11), (13) and (20) to (22) is used for cases that velocity data are obtained at enough high frequency.

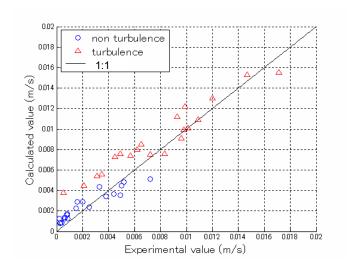


Figure 16. Comparison of pickup rates between experimental values and values calculated with instantaneous velocity.

## **CONCLUSIONS**

Influence of turbulence on sediment pickup rate was investigated. Relation between pickup rate and turbulence property of ambient flow was analyzed through a laboratory experiment. It was shown that the pickup rates with external turbulence generated by a grid structure were much larger than those for non-turbulent conditions. The pickup rates could be up to three times in the present study.

A new formula in which external turbulence was taken into account for Shields parameter evaluation was proposed. In the formula, excess drag force by turbulence acting on sediment particles was evaluated and inertia force caused by high frequency velocity variation was also included. The inertia force was considered to be minor, but should not be neglected.

Since the turbulence structure (or turbulence source) may affect the rate of pickup, further investigation is needed for various conditions of turbulence such as those under wave breaking.

#### **ACKNOWLEDGMENTS**

This research was partly supported by JSPS, Grant-in-Aid for Scientific Research(C), 21560534.

### **REFERENCES**

- Cheng, N.S., B.M. Sumer, and J. Fredsøe. 2003. Investigation of bed shear stresses subject to external turbulence, *International Journal of Heat and Fluid Flow*, 24, 816-824.
- Jones, W.P., and B.E. Launder. 1972. The prediction of laminarization with a two-equation model of turbulence, *International Journal of Heat Mass Transfer*, 15, 301-314.
- Nadaoka, K., S. Ueno, and T. Igarashi, 1988. Sediment suspension due to large scale eddies in the surf zone, *Proceedings of 21*<sup>st</sup> *International Conference on Coastal Engineering*,, ASCE, 1646-1660.
- Nielsen, P. 1992. Coastal bottom boundary layer and sediment transport, World Scientific, Singapore, 224-226.
- van Rijn, L.C. 1984. Sediment pick-up functions. *Journal of Hydraulic Engineering*, 110(10), 1494-1502.
- Sumi, H., T. Takae, and T. Nozaki. 2009. Experimental study on temporal and spatial distributions of bottom shear stresses in surf zone, *Journal of JSCE*, B2, 65(1), 101-105. (Japanese)
- Suzuki, T., A. Okayasu, and T. Shibayama. 2007. A numerical study of intermittent sediment concentration under breaking waves in the surf zone, *Coastal Engineering*, 54, 433-444.